

Highly non-Gaussian states created via cross-Kerr nonlinearity

Tomáš Tyc^{1,2} and Natalia Korolkova¹

¹ School of Physics and Astronomy, University of St Andrews, North Haugh, St Andrews, KY16 9SS, Scotland

²Institute of Theoretical Physics, Masaryk University, Kotlářská 2, 61137 Brno, Czech Republic

E-mail: tomtyc@physics.muni.cz

Abstract. We propose a feasible scheme for generation of strongly non-Gaussian states using the cross-Kerr nonlinearity. The resultant states are highly non-classical states of electromagnetic field and exhibit negativity of their Wigner function, sub-Poissonian photon statistics, and amplitude squeezing. Furthermore, the Wigner function has a distinctly pronounced “banana” or “crescent” shape specific for the Kerr-type interactions, which so far was not demonstrated experimentally. We show that creating and detecting such states should be possible with the present technology using electromagnetically induced transparency in a four-level atomic system in N-configuration.

PACS numbers: 42.65.-k, 42.50.-p, 03.67.-a

1. Introduction

Non-Gaussian and in general non-classical states of light enjoy an increasing interest in the quantum information community. They are indispensable building blocks for entanglement generation, distillation and broadcasting, for quantum information relays and networks in the realm of quantum information processing based on infinite-dimensional optical systems and atomic ensembles [1, 2]. As has been shown, it is impossible to perform optical quantum computation with linear optics only and a nonlinear interaction is needed to perform a universal quantum computation [3]. Hence it is unavoidable to investigate the nonlinearities of atomic systems or alternative solutions for giant nonlinearities and efficient nonlinear coupling, such as measurement-induced nonlinearities or other non-Gaussian operations. In addition, the experimental difficulty associated with the “on-line” nonlinear operations can be circumvented by using the off-line resources, the highly non-Gaussian states prepared separately from the actual computation and fed into the computation circuits when necessary to replace the nonlinear gates [4, 5]. Continuous-variable quantum repeaters, quantum relays and a number of other computation and communication tasks rely on non-Gaussian operations or non-Gaussian states, states described by a non-Gaussian Wigner function.

One of the examples of a non-linear coupling is the cross-Kerr effect which involves controlling the refractive index experienced by one mode of the electromagnetic field by the intensity of another. In this paper, we propose an experiment that employs the cross-Kerr effect to create highly non-classical non-Gaussian states of light via interaction of two coherent beams in an atomic medium exhibiting electromagnetically-induced transparency [6], subsequent measurement on one beam and feed-forward on the other. Such experiment on the one hand responds to the need for an efficient source of non-Gaussian states, on the other hand can be seen as a test-bench for the strong non-linear coupling using an EIT based system. In our case, the first evidence of the large non-linear phase shift in combination with enough coherence to generate and preserve quantum features can be obtained using merely a direct photodetection to verify the photon-number squeezing in one of the output modes. This would pave the way for further applications of such non-linear systems: Cross-Kerr nonlinear interaction provides a basis for several proposals of quantum information protocols or their elements, such as non-demolition photon number detection [7], C-NOT gate [8], or continuous-variable entanglement concentration [9, 10].

The first basic ingredient of our scheme is the nonlinear coupling based on the third-order nonlinearity, an optical cross-Kerr effect [11]. Such Kerr-type interaction of the two initially independent coherent beams a and b entangles them producing a continuous-variable state of modes a and b with quantum correlations between photon number in one mode and phase of the other. A subsequent measurement done on the mode b generates a conditional squeezed state of the mode a . This is a photon-number squeezed state described for the first time in [12]. The mechanism behind it is a re-shaping of the quantum uncertainty due to the Kerr-effect and the influence of a local measurement on the system of two spatially-separated entangled modes. A particular feature of the states squeezed using Kerr nonlinearity is their non-Gaussian character in contrast to the squeezed states produced, e.g., in the parametric process based on the nonlinearity of the second order [2]. The corresponding Wigner function has a specific crescent shape and exhibits negativity in some regions of the phase space in the form of the decaying fringes, resembling a section of the Wigner function of the Fock states. Indeed, there is a strong connection between the states emerging in this scheme and the Fock states: the generation of the non-classical state in our scheme can be understood as a superposition effect between different photon-number or Fock states. Hence the resultant Wigner function can be viewed a result of interference between the Fock-state Wigner functions with different photon numbers n . We will provide a more detailed discussion of the mechanism producing this particular state in Sec. 3 and 4 of the paper.

Another inherent feature of our protocol is the controlled displacement. We are dealing with continuous variable quantum systems. It means, that although in each single run of the proposed experiment (corresponding to a single measurement result on mode b) a squeezed state is created, the detection of squeezing will not be possible because it requires a statistical processing of an ensemble of measurement results. In

a number of subsequent runs, the overall squeezing vanishes, as we then will obtain a mixture of quantum uncertainties with different mean photon numbers and the overall state will become fuzzy. The way out is provided by the quantum feed-forward: the state in the mode a is displaced in each run with a displacement amplitude determined by a corresponding measurement outcome in mode b . This procedure merges all differently displaced crescent-shaped uncertainties into a single crescent which exhibits amplitude (or photon-number) squeezing.

The non-classical non-Gaussian states of this type have not yet been demonstrated experimentally although the Kerr effect, e.g. in optical nonlinear fibres, was exploited extensively for squeezing and entanglement generation (see e.g. [13, 14]). The challenging point is to produce the strong enough nonlinear coupling to generate sensible non-Gaussian features. All the experiments performed so far were working in the regime of weak nonlinearity restricting themselves to the first stages of quantum state evolution, which can be well approximated by the Gaussian Wigner function of the same type as the one describing squeezing in parametric second-order nonlinear processes. The most promising candidate for observing the large cross-Kerr effect is the four-level atomic medium exhibiting electromagnetically induced transparency (EIT) [6]. Under certain conditions, the cross-phase modulation in such media can reach values by many orders of magnitude larger than it is possible in optical fibres and the phase shift between two photons can reach values of 10^{-3} for hot atoms in a vapour cell or even 10^{-1} for cold atoms in a magneto-optical trap [15]. The experimental feasibility of achieving a large cross-Kerr interaction for continuous-wave fields has been demonstrated using cold atoms in magneto-optical trap [16]. Recently, a suitable method was suggested for group-velocity matched pulses and room temperature atomic gas cell [15]. The form of the cross-Kerr interaction in a such four-level atomic system in the N-configuration can be derived in a simple way [17]. Essentially, the strong cross-Kerr interaction is caused by the ac-Stark shift produced by the third perturbing field to the dark-state of the lambda subsystem.

The paper is organised as follows. In Sec. 2 we present the experimental scheme. Sec. 3 discusses the non-Gaussian properties of the state obtained in a single run of the experiment. In Sec. 4 we show how a controlled displacement on this output state can reproduce the same highly non-Gaussian state in multiple runs generating a constant output state with high accuracy. In Sec. 5 we discuss the scaling of the non-Gaussian effects with experimental parameters and conclude in Sec. 6.

2. Experimental scheme

Consider the following experimental scheme sketched in Figure 1: two coherent states with amplitudes α and β occupying modes a and b , respectively, interact in a cross-Kerr medium and mode b is then subject to a measurement of the \hat{x} quadrature via homodyne detection. Based on the measurement outcome x , a displacement operation is performed on mode a . In this section we obtain the form of the output state ρ and

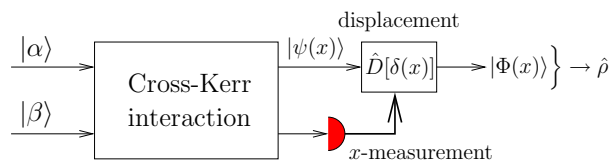


Figure 1. Proposed experimental setup for generating crescent states with negative Wigner function: two coherent states interact in a cross-Kerr medium, one of them is subject to measurement of the field quadrature, and displacement is performed on the other one depending on the measurement outcome.

its properties will be discussed in the following sections.

The Hamiltonian of the cross-Kerr interaction is

$$\hat{H} = -\gamma' \hat{n}_a \hat{n}_b, \quad (1)$$

where γ' expresses the strength of the interaction and $\hat{n}_a = \hat{a}^\dagger \hat{a}$, $\hat{n}_b = \hat{b}^\dagger \hat{b}$ are the photon number operators of the two modes. We introduce the phase shift between two photons as $\gamma = \gamma' t$, where t is the interaction time, which gives the evolution operator $\hat{U} = \exp(i\gamma \hat{n}_a \hat{n}_b)$. If the two modes are originally in coherent states $|\alpha\rangle_a$ and $|\beta\rangle_b$, then after the cross-Kerr interaction their state will be

$$\begin{aligned} |\Psi\rangle_{ab} &= \exp(\gamma \hat{n}_a \hat{n}_b) |\alpha\rangle_a |\beta\rangle_b = e^{-|\alpha|^2/2} \sum_{n=0}^{\infty} \frac{\alpha^n}{\sqrt{n!}} \exp(\gamma \hat{n}_a \hat{n}_b) |n\rangle_a |\beta\rangle_b \\ &= e^{-|\alpha|^2/2} \sum_{n=0}^{\infty} \frac{\alpha^n}{\sqrt{n!}} |n\rangle_a |\beta e^{i\gamma n}\rangle_b \end{aligned} \quad (2)$$

This is an entangled state where the photon number n_a in mode a is correlated with the amplitude of coherent state in mode b by introducing to it a phase shift dependent on n_a (and vice versa).

In the next step the quadrature $\hat{x} = (\hat{b} + \hat{b}^\dagger)/\sqrt{2}$ of mode b is measured via homodyne detection with the outcome x , which results in the following (unnormalized) state of mode a :

$$|\psi(x)\rangle_a = {}_b\langle x | \Psi \rangle_{ab} = \frac{e^{-|\alpha|^2/2}}{\sqrt[4]{\pi}} \sum_{n=0}^{\infty} \frac{\alpha^n \exp[-(x - \sqrt{2}\beta_n)^2/2 + i\sqrt{2}\beta'_n x - i\beta_n \beta'_n]}{\sqrt{n!}} |n\rangle_a \quad (3)$$

where we have denoted $\beta_n = \text{Re}(\beta e^{i\gamma n})$, $\beta'_n = \text{Im}(\beta e^{i\gamma n})$ and used the expression for a coherent state in x -representation. The square of the norm of $|\psi(x)\rangle_a$ is the probability density $P(x)$ that the particular measurement outcome x occurs.

As the last step, a displacement in the phase space is applied to mode a . The resulting state of mode a is then

$$|\Phi(x)\rangle = \hat{D}[d(x)] |\psi(x)\rangle = e^{d(x)\hat{a}^\dagger - d^*(x)\hat{a}} |\psi(x)\rangle, \quad (4)$$

where $d(x)$ is the displacement parameter that depends on the measurement outcome x . When the experiment is performed repeatedly, then the output state is averaged to

$$\hat{\rho} = \int_{\mathbb{R}} |\Phi(x)\rangle \langle \Phi(x)| dx, \quad (5)$$

which is properly normalized.

The state $|\Phi(x)\rangle$ in general depends on the measurement outcome x . However, we will show that in a certain regime this dependence can be quite weak. This way, by running the experiment many times (and obtaining different values of x), one can still get almost a pure state $\hat{\rho}$ at the output mode a that has highly non-classical properties.

3. Properties of the state $|\psi(x)\rangle$

Before describing the averaged output state $\hat{\rho}$, in this section we will focus on the state $|\psi(x)\rangle$ of mode a after the \hat{x} measurement on mode b has been performed. Consider the specific situation of $\beta = i|\beta|e^{-i\gamma|\alpha|^2}$, i.e., when the phase of the mode b is set to $\pi/2 - \gamma|\alpha|^2$. We also put a constraint on $|\alpha|$, such that $|\alpha| \leq 10$ and the product $|\alpha\beta|\gamma$ is of order of unity. The reasons for these assumptions will be explained later in this section. Taking into account that γ is several orders of magnitude smaller than unity, it also holds that $\gamma|\alpha| \ll 1$.

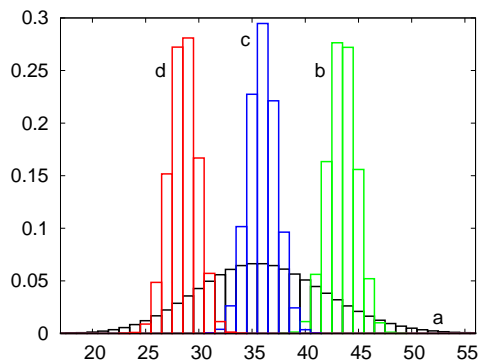


Figure 2. Photon number probability distribution of the coherent state $|\alpha\rangle$ (a, black curve) compared with the normalized distributions of the states $|\psi(x)\rangle$. The parameters are $|\alpha| = 6$, $\gamma|\beta| = 0.36$ and $x = -4$ (b, green curve), $x = 0$ (c, blue curve) and $x = 4$ (d, red curve). The photon number distribution in the states $|\psi(x)\rangle$ is about $4\times$ squeezed compared to the Poissonian statistics of the coherent state $|\alpha\rangle$.

In this particular case, for evaluating the real and imaginary parts of $\beta e^{i\gamma n}$ to calculate β_n and β'_n in (3), we use the expansion of the exponential function as follows:

$$\beta e^{i\gamma n} = i|\beta|e^{i\gamma(n-|\alpha|^2)} \approx i|\beta| - \gamma|\beta|(n - |\alpha|^2). \quad (6)$$

We terminated the series after the second term since $\gamma(n - |\alpha|^2) \ll 1$ for all n for which the probability of having n photons in the state $|\alpha\rangle$ is non-negligible. Indeed, the photon number distribution of the state $|\alpha\rangle$ is Poissonian with both mean and variance equal to $|\alpha|^2$, hence $(n - |\alpha|^2)$ is of order of $|\alpha|$ and therefore $\gamma(n - |\alpha|^2) \ll 1$ holds in agreement with our assumption $\gamma|\alpha| \ll 1$.

From (6) we get $\beta_n = -|\beta|\gamma(n - |\alpha|^2)$ and $\beta'_n = |\beta|$. Substituting this into (3) we

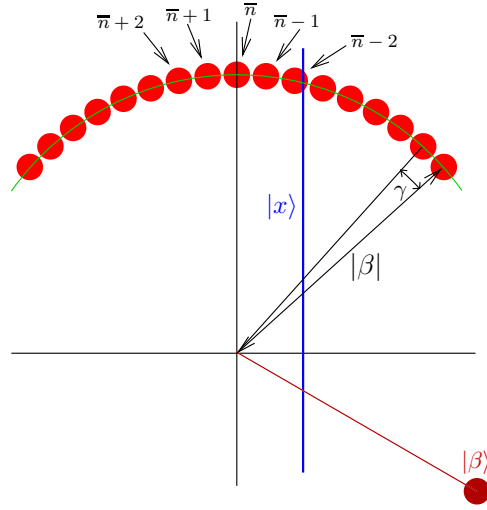


Figure 3. Illustration in the phase space of how the photon number squeezing of the state $|\psi(x)\rangle$ emerges: the red circles represent the uncertainty regions of coherent states $|e^{i\gamma n}\beta\rangle_b$ in (2) entangled with the photon numbers n in mode a ($\bar{n} \approx |\alpha|^2$ denotes the most likely photon number). The circles are distributed along the green arch centred at the origin of the phase space, having the radius $|\beta|$ and stretching to the angle of approximately $\gamma|\alpha|$ to both sides of the imaginary axis. If then the quadrature \hat{x} is measured on mode b with a particular outcome x (blue line represents the quadrature eigenstate $|x\rangle$), then only those states are chosen from the superposition (3) that have a non-negligible overlap with $|x\rangle$. If the length of the arch, $2\gamma|\alpha\beta|$, is larger than the spatial extension of the uncertainty region of about unity, then only a relatively small number of circles have a significant overlap with $|x\rangle$ and so the photon number variance in the state $|\psi(x)\rangle$ is reduced significantly compared to the state $|\alpha\rangle$. The effect is the strongest when the arch is, very loosely speaking, perpendicular to the line representing $|x\rangle$; this gives the phase condition on β .

arrive at

$$|\psi(x)\rangle = \frac{e^{i\phi - |\alpha|^2/2}}{\sqrt[4]{\pi}} \sum_{n=0}^{\infty} \frac{\alpha^n}{\sqrt{n!}} \exp \left[i\gamma|\beta|^2 n - \gamma^2|\beta|^2 \left(n - |\alpha|^2 + \frac{x}{\sqrt{2}|\beta|\gamma} \right)^2 \right] |n\rangle, \quad (7)$$

where $\phi = \sqrt{2}x|\beta| + \gamma|\alpha\beta|^2$ is an irrelevant global phase factor. The important term here is the exponent, which provides the insight into the main physical effects due the cross-Kerr interaction. The first term in the exponent shows that the phase of the state $|\psi(x)\rangle$ is increased by $\gamma|\beta|^2$ with respect to the phase of the original state $|\alpha\rangle$. The second, Gaussian term causes the photon number distribution in $|\psi(x)\rangle$ to be altered with respect to the original Poissonian distribution of the state $|\alpha\rangle$: If $2|\alpha\beta|\gamma > 1$, then this term becomes more important than the factor $\alpha^n/\sqrt{n!}$. Moreover, as the product $2|\alpha\beta|\gamma$ grows above unity, the photon number distribution quickly gets dominated by the Gaussian term. In this situation the mean photon number is $|\alpha|^2 - x/(\sqrt{2}|\beta|\gamma)$ compared to $|\alpha|^2$ for the coherent state $|\alpha\rangle$ and the variance of the photon number distribution is $1/(2\gamma|\beta|)^2$ compared to $|\alpha|^2$ for $|\alpha\rangle$. This means that the state $|\psi(x)\rangle$ is squeezed in the photon number by the factor of approximately $2|\alpha\beta|\gamma$, as illustrated

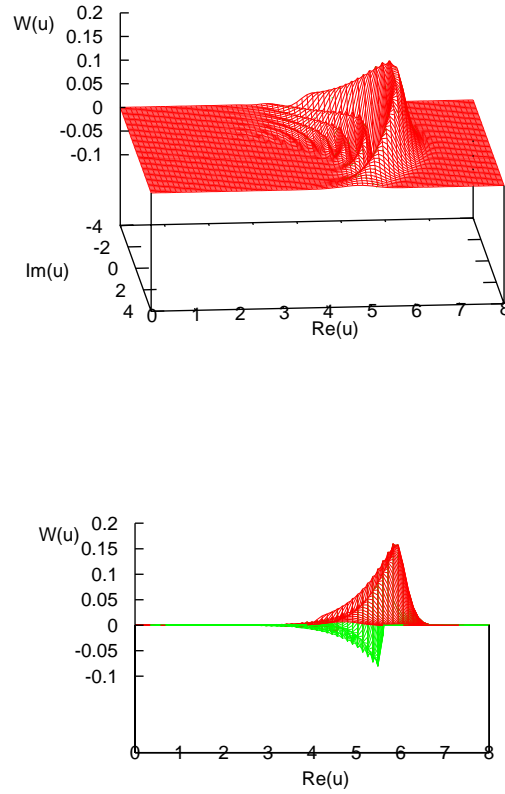


Figure 4. Two different views of the Wigner function $W(u)$ of the output state $|\psi(x)\rangle$ for $|\alpha| = 6$, $\gamma|\beta| = 0.36$ and $x = 0$. The product $|\alpha\beta\gamma|$ is equal to 2.16 and the phase of α is set to $-\gamma|\beta|^2$ to make the phase of the output state zero. The crescent shape and negative values of the Wigner function are clearly visible.

in Figure 2 for $|\alpha\beta\gamma| \approx 2.16$ and different values of the measurement result x . Thus if $2|\alpha\beta\gamma| > 1$, then the output state will exhibit a strongly sub-Poissonian photon statistics. Figure 3 gives a visualisation of the above argumentation. Equation (7) and Figure 3 also provide an argument for the particular choice of the phase of the mode b , $\beta = i|\beta|e^{-i\gamma|\alpha|^2}$. This way we have demonstrated the photon number variance reduction – photon number squeezing in the output state $|\psi(x)\rangle$ obtained in a single run of the experiment. A consequence of this reduction are several non-classical phenomena: negativity and crescent shape of the Wigner function, as well as amplitude squeezing.

Figures 4 and 5 show the Wigner function corresponding to the output state $|\psi(x)\rangle$ of (7) for different values of $|\alpha|$ and $\gamma|\beta|$. The above mentioned features of the Wigner function are clearly visible especially in Figure 4. Comparison of Figures 4 and 5 provides a clear insight into the assumptions made in the beginning of this section. For large values of $|\alpha|$ (say over 10) one gets a state that is close to a squeezed Gaussian state

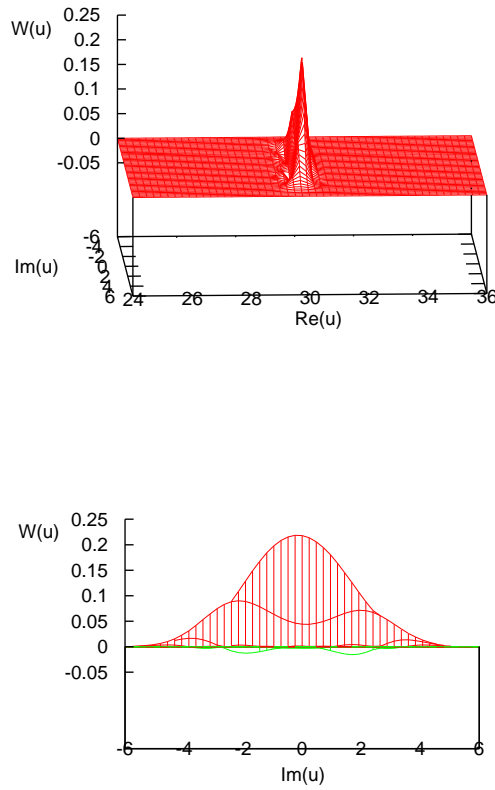


Figure 5. Two different views of the Wigner function $W(u)$ of the output state $|\psi(x)\rangle$ for $|\alpha| = 30$, $\gamma|\beta| = 0.066$ and $x = 0$ such that $|\alpha\beta\gamma| = 1.98$. The state is strongly squeezed and is close to a Gaussian state, hence the negativeness of the Wigner function is weak.

and the features we are looking for, namely the negativity and crescent-shape of the Wigner function, are suppressed (Figure 5). We also assumed that the product $|\alpha\beta|\gamma$ is of order of unity because otherwise the photon number squeezing is small, the state $|\psi(x)\rangle$ is close to a coherent state and hence does not have strong non-Gaussian and non-classical properties. $|\alpha\beta|\gamma > 1$ requires a large cross-Kerr nonlinearity and/or a large amplitude β . The former we anticipate to be feasible with the four-level EIT based system mentioned in the Introduction. The Wigner function in Figure 4 is plotted for the parameters satisfying all the discussed restrictions, with $|\alpha\beta|\gamma \approx 2.16$ as in Figure 2. Such features as the negativity and crescent-shape are highly pronounced, confirming the strongly non-Gaussian character of the output state.

4. Effect of displacement in the phase space

As we have seen, the output state $|\psi(x)\rangle$ depends on the value x obtained by the measurement. Specifically, for different x , there will be different mean photon numbers in the output state of the mode a . To prepare an identical crescent state repeatedly, one strategy would be to post-select the output at some sufficiently narrow interval of x , which would, however, reduce the success rate significantly. Another option, however, is to correct for the change of the mean photon number caused by the x -measurement. It turns out that this correction can be achieved with a good accuracy by performing a phase-space displacement operation $\hat{D}[(d(x))]$ with displacement parameter d depending on x . In this way one can obtain a state $|\Phi(x)\rangle$ almost independent of the measurement outcome x , which makes $\hat{\rho}$ in (5), Figure 1 nearly a pure state.

To find the displacement magnitude $|d(x)|$ that would compensate for the change of the mean photon number, we recall that for coherent states, the mean photon number depends quadratically on the amplitude. The state $|\psi(x)\rangle$ has the mean photon number $|\alpha|^2 - x/(\sqrt{2}|\beta|\gamma)$ and therefore its mean amplitude $|\alpha'|$ is equal to the square root of this number. In order to revert to the original amplitude $|\alpha|$, we need to displace by $|\alpha| - |\alpha'|$. The direction of the displacement in the phase space is given by the phase of the state $|\psi(x)\rangle$, which is, as seen from (7), equal to $\gamma|\beta|^2 + \arg(\alpha)$. This way we arrive at the displacement parameter

$$d(x) = \left(|\alpha| - \sqrt{|\alpha|^2 - \frac{x}{\sqrt{2}\gamma|\beta|}} \right) e^{i[\gamma|\beta|^2 + \arg(\alpha)]}. \quad (8)$$

To see that the state $|\Phi(x)\rangle$ in (4) is really almost independent of the measurement outcome x , we investigate the normalized scalar product

$$F(x) \equiv \frac{\langle \Phi(0) | \Phi(x) \rangle}{\sqrt{\langle \Phi(0) | \Phi(0) \rangle \langle \Phi(x) | \Phi(x) \rangle}} \quad (9)$$

that expresses the overlap of the displaced output state corresponding to an arbitrary x and the one corresponding to $x = 0$. Figure 6 shows the function $F(x)$ and the probability density $P(x) = \langle \psi(x) | \psi(x) \rangle$ of the quadrature for a few values of $|\alpha|$ and $\gamma|\beta|$. It can be seen that in the regions of x where the probability $P(x)$ is non-negligible, the function $F(x)$ has values close to unity, and this is a typical behaviour. This means that the state $|\Phi(x)\rangle$ is close to $|\Phi(0)\rangle$ for all x that are likely to be found in the quadrature measurement. Therefore $\hat{\rho}$, which is the mixture of these states [see (5)], will be almost a pure state. Numerical simulations confirm this and the purity $\mathcal{P} = \text{Tr } \hat{\rho}^2$ has values of approximately 0.95 for the states corresponding to parameters α, β and γ in Figures 4 and 5.

Experimentally, the desired controlled displacement can be realized mixing the state $|\psi(x)\rangle$ with a coherent state $|d/t\rangle$ on a beam splitter with a very low transmissivity t . If $|t| \ll 1$, then one obtains almost exactly the state $\hat{D}(d)|\psi(x)\rangle$ at one beam splitter output port [18]. The amplitude d/t can be varied electronically according to the measured value x and (8) using, e.g., the scheme depicted in Figure 7.

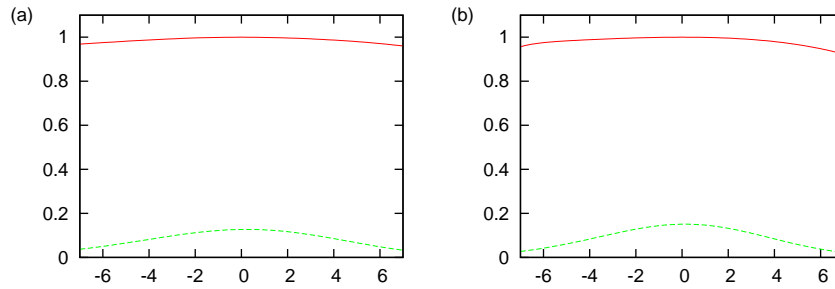


Figure 6. The normalized scalar product $F(x)$ (solid red line) and the probability density $P(x)$ (dashed green line) as a function of x for (a) $|\alpha| = 6, \gamma|\beta| = 0.36$ and (b) $|\alpha| = 9, \gamma|\beta| = 0.2$. Since the function $F(x)$ is much broader than $P(x)$, the fidelity $F(x)$ is almost unity for all values x likely to be found in the measurement, and therefore the state $|\Phi(x)\rangle$ is almost independent of x .

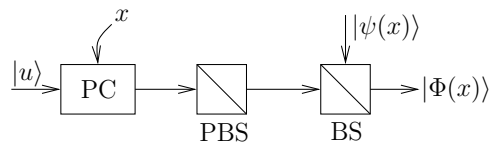


Figure 7. A possible way of realizing the displacement operation: a vertically polarised coherent beam is directed into a Pockels cell (PC) with the optical axis rotated by 45 degrees and controlled by the outcome x of quadrature measurement. The output beam then impinges onto a polarising beam splitter (PBS), which yields a polarised coherent beam with amplitude depending on x . This beam is then mixed with the state $|\psi(x)\rangle$ on a highly reflective beam splitter (BS). The displaced state $|\Phi(x)\rangle$ is found at one output.

5. Scaling of the non-classical effects with $|\alpha|, |\beta|$ and γ

In what follows, we discuss the scaling of the effects described above for the output state $|\Phi(0)\rangle = |\psi(0)\rangle$, as we have shown that the state $|\Phi(x)\rangle$ is almost independent of x . An inspection of formulas (7) and (8) shows that, apart from phase factors, the form of the output states depends on $|\alpha|$ and the product $\gamma|\beta|$.

Consider first the effect of varying $\gamma|\beta|$ while keeping $|\alpha|$ constant. For $\gamma|\beta| = 0$, the output state reduces to the original state $|\alpha\rangle$. For very small $\gamma|\beta|$ for which $\gamma|\alpha\beta| \ll 1$, the state $|\psi(0)\rangle$ is close to a weakly squeezed coherent state with amplitude $\alpha \exp(i\gamma|\beta|^2)$, so it is almost Gaussian. As $\gamma|\beta|$ increases, $|\psi(0)\rangle$ starts to deviate from a Gaussian state, negative regions of the Wigner functions get larger, and the crescent shape of $|\psi(0)\rangle$ emerges, as well as the photon number squeezing. When $\gamma|\beta|$ gets larger than unity, $|\psi(x)\rangle$ is almost a Fock state $|n\rangle$ with photon number n depending on the measured value of x , and it is no longer true that $|\Phi(x)\rangle$ is almost independent of x . In this situation our scheme (without the displacement operation) can be used as a conditional source of Fock states.

The effect of varying α while keeping the product $\gamma|\alpha\beta|$ constant is different. The

phase of α influences just the phase of $|\psi(0)\rangle$. If $|\alpha|$ is small, the crescent shape of the Wigner function is strongly pronounced, as well as its negativeness, because the state is squeezed in photon number and is not far from a Fock state. Close to the origin of the phase space the circles corresponding to a fixed photon number are more curved than those farther from the origin, and hence the Wigner function corresponding to smaller $|\alpha|$ shows a stronger crescent shape than the one corresponding to larger $|\alpha|$. In contrast, for larger $|\alpha|$ the state is closer to a Gaussian state whose Wigner function is positive. Hence the negativeness of the Wigner function is more profound in case of smaller $|\alpha|$, and this case is more appealing experimentally. Figures 4 – 5 illustrate this behaviour.

6. Conclusion

In conclusion, we have suggested a feasible scheme to generate highly non-Gaussian states exhibiting crescent-shaped Wigner function with negative regions. We envisage the application of such states in quantum information processing using infinitely-dimensional, continuous-variable quantum systems. The non-Gaussian operations and non-Gaussian states attract currently an increasing attention in this context (see e.g. [4, 19] and references therein) and there is a high demand in the community for their experimentally viable implementation. In our scheme, the initial states as well as the detection (Figure 1), feed-forward (Figure 7) and evaluation steps belong to the standard toolbox of quantum optics and are readily available in the laboratory. The first verification of quantum features can be performed with merely direct photodetection to prove the photon-number squeezing of Fig 2. The negativity of the Wigner function and its crescent shape can be visualised using quantum state tomography [20], a more involved but established procedure [21, 22]. For the first demonstration of the effect using the tomographic measurement of the Wigner function of the state $\hat{\rho}$, the displacement operation of Figure 7 can be simplified via replacing it by the electronic one.

The challenging part of the proposed scheme is the strong nonlinear coupling implied. Again, it represents an important building block in quantum information processing attracting recently a substantial interest from both the theoretical and experimental sides. A feasible nonlinear coupling device would make a profound impact on the development of quantum communication and computation protocols. So far, there are only few first quite involved implementations demonstrating this effect [16], [23]. For the realization of our scheme, we suggest the nonlinear optical cross-Kerr effect in an EIT based four-level atomic system, which was closely studied recently both theoretically [6, 15, 17, 24] and experimentally [16]. Furthermore, due to the experimental availability of the other elements and particular simplicity of the first verification using direct photodetection, our suggested scheme can serve as a test bench for the strong nonlinear coupling preserving quantum effects.

Acknowledgments

We thank Friedrich König and Chris Kukulicz for valuable discussions. We gratefully acknowledge the financial support of the EU project COVAQIAL (FP6-511004) under STREP and of the Leverhulme Trust.

- [1] Cerf N, Leuchs G and Polzik E S (eds.) 2007 *Quantum Information with Continuous Variables of Atoms and Light* (Imperial College Press)
- [2] Dell'Anno F, De Siena S and Illuminati F 2006 *Phys. Rep.* **428** 53 and references therein
- [3] Lloyd S and Braunstein S L 1999 *Phys. Rev. Lett.* **82** 1784
- [4] Ghose S and Sanders B C 2007 *J. Mod. Opt.* **54** 855
- [5] Ralph T C, Gilchrist A, Milburn G J, Munro W J and Glancy S 2003 *Phys. Rev. A* **68** 042319
- [6] Schmidt H and Imamoglu A 1996 *Opt. Lett.* **21** 1936
- [7] Beausoleil R G, Spiller T P, Munro W J and Nemoto K 2005 *Phys. Rev. A* **71** 033819
- [8] Munro W J, Nemoto K and Spiller T P 2007 *New J. Phys.* **7** 137
- [9] Fiurásek J, Filip R and Mišta L 2003 *Phys. Rev. A* **67** 022304
- [10] Menzies D and Korolkova N 2006 *Phys. Rev. A* **74** 042315
- [11] Shen Y R 1984 *The Principles of Nonlinear Optics* (J Wiley, Hoboken)
- [12] Kitagawa M and Yamamoto Y 1986 *Phys. Rev. A* **34** 3974
- [13] Silberhorn Ch, Lam P K, Weiß O, König F, Korolkova N and Leuchs G 2001 *Phys. Rev. Lett.* **86** 4267
- [14] Heersink J, Gaber T, Lorenz S, Glöckl O, Korolkova N and Leuchs G 2003 *Phys. Rev. A* **68** 013815
- [15] Wang Z B, Marzlin K-P and Sanders B C 2006 *Phys. Rev. Lett.* **97** 063901
- [16] Kang H and Zhu Y 2003 *Phys. Rev. Lett.* **91** 093601
- [17] Sinclair G and Korolkova N 2007, to appear in *Phys. Rev. A*
- [18] Furusawa A, Sørensen J L, Braunstein S L, Fuchs C A, Kimble H J and Polzik E S 1998, *Science* **282** 706
- [19] Genoni M G, Paris M G A and Banaszek K 2007 *Preprint* 0704.0639; Dell'Anno F, De Siena S, Albano Farias L and Illuminati F 2007 *Phys. Rev. A* **76** 022301; Mølmer K 2006 *Phys. Rev. A* **73** 063804; Heersink J, Marquardt Ch, Dong R, Filip R, Lorenz S, Leuchs G, and Andersen U L 2006 *Phys. Rev. Lett.* **96** 253601
- [20] Leonhardt U, Munroe M, Kiss T, Richter Th and Raymer M G 1996 *Opt. Commun.* **127** 144; Leonhardt U 2003 *Measuring the Quantum State of Light* (Cambridge University Press, Cambridge)
- [21] Lvovsky A I and Raymer M G 2007 "Continuous-variable quantum-state tomography of optical field and photons" in *Quantum Information with Continuous Variables of Atoms and Light* (Imperial College Press)
- [22] Breitenbach G, Schiller S and Mlynek J 1997 *Nature* **387** 471
- [23] Roos C F, Monz T, Kim K, Riebe M, Haeflner H, James D F V and Blatt R 2007 *Preprint* 0705.0788
- [24] Beausoleil R G, Munro W J and Spiller T P 2004 *J. Mod. Opt.* **51** 1559; Beausoleil R G, Munro W J, Rodrigues D A and Spiller T P 2004 *J. Mod. Opt.* **51** 2441